

Title	Thermodynamic Properties of Tetra-n-butylphosphonium Dicarboxylate Semiclathrate Hydrates
Author(s)	Shimada, Jin; Yamada, Moe; Tani, Atsushi et al.
Citation	Journal of Chemical and Engineering Data. 2022, 67(1), p. 67-73
Version Type	AM
URL	<a href="https://hdl.handle.net/11094/91292">https://hdl.handle.net/11094/91292</a>
rights	This document is the Accepted Manuscript version of a Published Work that appeared in final form in Journal of Chemical and Engineering Data, © American Chemical Society after peer review and technical editing by the publisher. To access the final edited and published work see <a href="https://doi.org/10.1021/acs.jced.1c00741">https://doi.org/10.1021/acs.jced.1c00741</a> .
Note	

***Osaka University Knowledge Archive : OUKA***

<https://ir.library.osaka-u.ac.jp/>

Osaka University

# **Thermodynamic Properties of Tetra-*n*-butylphosphonium Dicarboxylate Semiclathrate Hydrates**

Jin Shimada<sup>1,2,3,4</sup>, Moe Yamada<sup>5</sup>, Atsushi Tani<sup>3</sup>, Takeshi Sugahara<sup>1,2,\*</sup>, Katsuhiko Tsunashima<sup>6,\*\*</sup>,  
Yusuke Tsuchida<sup>4,5,7</sup>, Takayuki Hirai<sup>1,2</sup>

<sup>1</sup>Division of Chemical Engineering, Department of Materials Engineering Science, Graduate School of Engineering Science, Osaka University, 1-3 Machikaneyama, Toyonaka, Osaka 560-8531, Japan

<sup>2</sup>Division of Energy and Photochemical Engineering, Research Center for Solar Energy Chemistry, Graduate School of Engineering Science, Osaka University, 1-3 Machikaneyama, Toyonaka, Osaka 560-8531, Japan

<sup>3</sup>Department of Human Environmental Science, Graduate School of Human Development and Environment, Kobe University, 3-11 Tsurukabuto, Nada, Kobe, Hyogo 657-8501, Japan

<sup>4</sup>Research Fellow of Japan Society for the Promotion of Science

<sup>5</sup>Department of Material Science, National Institute of Technology, Wakayama Collage, 77 Noshima, Nada, Gobo, Wakayama 644-0023, Japan

<sup>6</sup>Department of Applied Chemistry and Biochemistry, National Institute of Technology, Wakayama Collage, 77 Noshima, Nada, Gobo, Wakayama 644-0023, Japan

<sup>7</sup>Graduate School of Environmental and Information Sciences, Yokohama National University, 79-2

Tokiwadai, Hodogaya-ku, Yokohama, Kanagawa 240-8501, Japan

Corresponding Authors

\*(T.S.) Tel and Fax: +81-6-6850-6293. E-mail: [sugahara@cheng.es.osaka-u.ac.jp](mailto:sugahara@cheng.es.osaka-u.ac.jp)

\*\* (K.T.) Tel: +81-738-29-8413. Fax: +81-738-29-8439. E-mail: [tsunashima@wakayama-nct.ac.jp](mailto:tsunashima@wakayama-nct.ac.jp)

ORCID

Jin Shimada: 0000-0002-9720-5963

Atsushi Tani: 0000-0001-5788-2137

Takeshi Sugahara: 0000-0002-5236-5605

Katsuhiko Tsunashima: 0000-0002-4563-351X

Yusuke Tsuchida: 0000-0002-0016-5716

Takayuki Hirai: 0000-0003-4747-4919

## ABSTRACT

Semiclathrate hydrate (SCH) is one of the phase change materials suitable for cold energy storage. Thermodynamic properties of SCH, such as an equilibrium temperature and a dissociation enthalpy, depend on the size and shape of the guest substances. In the present study, to reveal the effects of steric conformation of the guest anions on the thermodynamic properties of SCHs, tetra-*n*-butylphosphonium dicarboxylate (TBP-DC) SCHs, where the anion was oxalate (TBP-Oxa), malonate (TBP-Mal), succinate (TBP-Suc), glutarate (TBP-Glu), maleate (TBP-Male), or fumarate (TBP-Fum), were investigated. TBP-Oxa, -Mal, -Suc, and -Fum SCHs had similar equilibrium temperatures, whereas the equilibrium temperatures of TBP-Glu and -Male SCHs were higher than those. It suggests that the size and conformation of glutarate and maleate anions are appropriate for the cage structures of SCHs. Moreover, we compared the equilibrium temperatures of TBP-Suc, -Male, -and -Fum SCHs because TBP-Suc, -Male, -and -Fum have similar anion structures. The equilibrium temperature of TBP-Suc SCH was similar to that of TBP-Fum SCH, whereas TBP-Male SCH showed higher equilibrium temperature. This result implies that the succinate anion is accommodated in the *trans* conformation, similar to the fumarate anion, in the hydrate cages.

## 1. Introduction

In recent years, demand for reducing greenhouse gas emission and energy conservation have been internationally growing. It is essential to develop technologies for efficient utilization of thermal energy, because a large amount of unused thermal energy is exhausted to the environment. Phase change materials (PCMs), which can utilize a latent heat, are promising for unused thermal energy storage. PCMs can not only store the unused thermal energy exhausted to the environment, but also contribute to fill the gap between electric power generation and demand. Ice is one of the most widely used PCMs at temperatures around 273 K. However, the equilibrium temperature of the ice is quite low for air conditioning and storage system for fresh foods.

A promising candidate for PCMs is a semiclathrate hydrate (SCH), which is a crystalline inclusion compound consisting of host water molecules and appropriate guest substances. Either quaternary alkyl ammonium or phosphonium salt has been used as the guest substances of SCHs. The cations are enclathrated in conjunct polyhedral cages and the anions participate in the hydrogen-bonded networks with host water molecules.<sup>1-4</sup> SCHs are expected as PCMs due to their unique thermodynamic properties, such as the equilibrium temperature located below 300 K and the relatively large dissociation enthalpy ( $160\text{--}220\text{ J}\cdot\text{g}^{-1}$ ) at atmospheric pressure.<sup>5-14</sup>

It is well known that the thermodynamic and crystallographic properties of SCHs depend on the chemical structures of guest substances<sup>5, 8-10, 14-16</sup>, in other words, there is designability of the SCHs

with desired thermodynamic and crystallographic properties by choosing appropriate guest substances.

Although the relations between the chemical structures of guest substances and the thermodynamic properties of SCHs have been studied, more detailed understandings are necessary to achieve the development of the SCHs suitable for PCMs. Many guest substances have been studied; *i.e.* cations<sup>14-16</sup>, carboxylate anions<sup>5, 8-10, 12, 17-19</sup>, and unsaturated bond effects on cations and anions<sup>5, 12, 14, 18</sup>.

Although simple effects of guest substances, such as alkyl size and anion species, have been studied, the effects of steric conformation of the guest substances have not been investigated. To control the thermodynamic properties of SCHs more precisely, detailed studies of conformation are essential.

Nakayama and Watanabe revealed the relations between the equilibrium temperature and composition of tetra-*n*-butylammonium dicarboxylate (TBA-DC) SCH systems<sup>20</sup>. In the Ref. [20], the effects of functional groups and the methylene chain of dicarboxylate anions on the equilibrium temperatures were also studied. Dyadin *et al.* reported the equilibrium temperatures and crystallographic properties of TBA-DC SCH systems.<sup>19, 21</sup> Recently, Arai *et al.* and Miyamoto *et al.* reported the phase equilibrium relations and dissociation enthalpies of tetra-*n*-butylphosphonium sulfate and tetra-*n*-butylphosphonium oxalate (TBP-Oxa) SCHs, respectively.<sup>11, 13</sup> The other equilibrium data of TBP-DC SCHs have not been reported.

In the present study, how the dicarboxylate anions with phosphonium cation, tetra-*n*-butylphosphonium dicarboxylates (TBP-DCs), affect the thermodynamic properties of SCHs were

studied. Oxalate (TBP-Oxa), malonate (TBP-Mal), succinate (TBP-Suc), glutarate (TBP-Glu), maleate (TBP-Male), and fumarate (TBP-Fum) anions were selected as the guest dicarboxylate anions.

The chemical structures of the dicarboxylate anions used in the present study were shown in **Figure 1**.

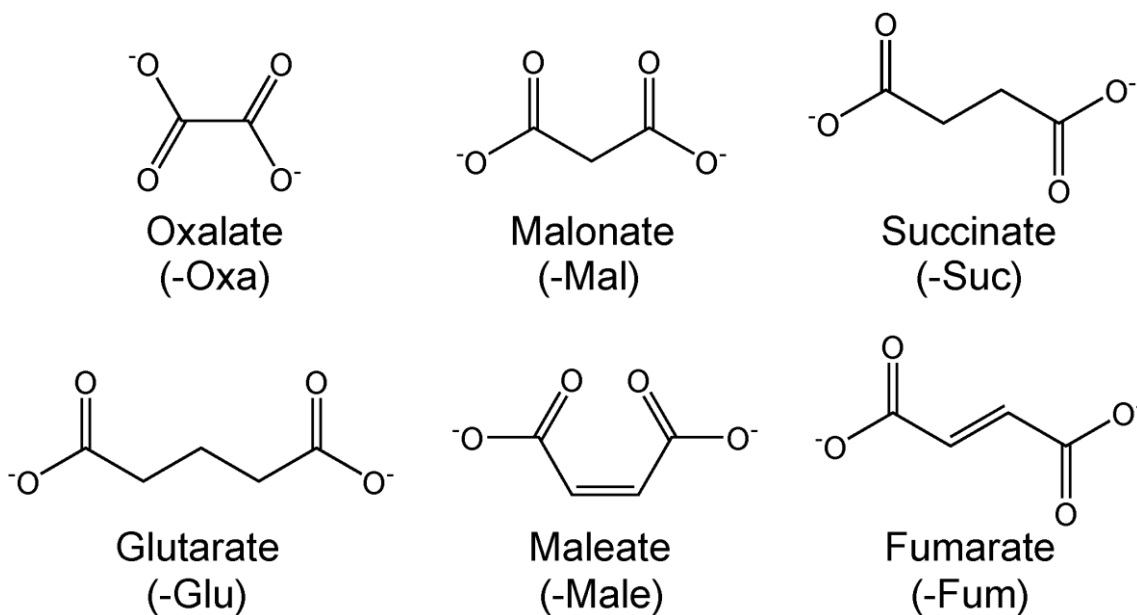


**Figure 1.** Chemical structures of the dicarboxylate anions used in the present study.

## 2. Experimental

### 2.1 Materials

The chemicals used in the present study were listed in **Table 1**. Each TBP-DC salt was synthesized by neutralization reaction between tetra-*n*-butylphosphonium hydroxide and the corresponding dicarboxylic acid in the aqueous solvent. The products were confirmed by  $^1\text{H}$ ,  $^{13}\text{C}$ , and  $^{31}\text{P}$  nuclear magnetic resonance (NMR) measurements (Bruker, AVANCE400). From NMR results, there were no impurity-derived signals or aberrant integration ratio. The purities of the synthesized TBP-DC salts

were higher than or equal to those originally included in the synthetic reagents. Majority of the impurity, considering the synthetic pathway, would be tri-*n*-butylphosphine oxide derivatives.



**Table 1.** Information on chemicals used in the present study.

Chemical name	CAS Reg. No.	Source	Mass fraction purity
tetra- <i>n</i> -butylphosphonium hydroxide	14518-69-5	Tokyo Chemical Industry Co., Ltd.	0.402 mass fraction in aqueous solution
oxalic acid	6153-56-6	FUJIFILM Wako Pure Chemical Corp.	> 0.995 (dihydrate)
malonic acid	141-82-2	FUJIFILM Wako Pure Chemical Corp.	> 0.98
succinic acid	110-15-6	Tokyo Chemical Industry Co., Ltd.	> 0.99
glutaric acid	110-94-1	Tokyo Chemical Industry Co., Ltd.	> 0.99
maleic acid	110-16-7	Tokyo Chemical Industry Co., Ltd.	> 0.99
fumaric acid	110-17-8	Tokyo Chemical Industry Co., Ltd.	> 0.99
water	7732-18-5	distilled and deionized	resistivity is 0.46 MΩ cm

## 2.2 Apparatus and procedures

The approximately 1 cm<sup>3</sup> of aqueous solutions were prepared at different compositions from  $x = 0.0016\text{--}0.0289$  ( $w = 0.0498\text{--}0.5004$ ) for TBP-Oxa,  $x = 0.0016\text{--}0.0284$  ( $w = 0.0515\text{--}0.5018$ ) for TBP-Mal,  $x = 0.0015\text{--}0.0275$  ( $w = 0.0498\text{--}0.4994$ ) for TBP-Suc,  $x = 0.0013\text{--}0.0276$  ( $w = 0.0450\text{--}0.5056$ ) for TBP-Glu,  $x = 0.0016\text{--}0.0276$  ( $w = 0.0535\text{--}0.4993$ ) for TBP-Male, and  $x = 0.0015\text{--}0.0279$  ( $w = 0.0502\text{--}0.5022$ ) for TBP-Fum with the electric balance (Sartorius, Secura 224-1S) with an uncertainty of 0.1 mg. The symbols  $x$  and  $w$  represent the mole and mass fractions, respectively. TBP-DC SCH samples were formed in a glass vials at 250 K. The vials were put in a propylene glycol bath thermostated with a cooling water circulator at 268 K (Taitec, CL-80R and EYELA, NCB-3100), and the system temperature was elevated with a step of 0.1 K. While the temperature was kept for 5 hours at each temperature, the glass vials were often shaken by hands. The equilibrium temperature was determined when the hydrate crystal was dissolved completely. The system temperature was measured by a platinum resistance thermometer (the uncertainty of 0.1 K) calibrated with the thermistor thermometer (Takara, D632, reproducibility: 0.02 K. The probe was calibrated with a Pt resistance thermometer defined by ITS-90). The hydration number ( $n$ ) of each TBP-DC SCHs was estimated from the composition at the maximum equilibrium temperature and the largest dissociation enthalpy. To determine them, apparent dissociation enthalpies per unit mass of aqueous solution were measured with differential scanning calorimetry. The value of apparent dissociation enthalpy reaches to the

maximum at the stoichiometric composition<sup>10, 12</sup>, because the excess amount of water or phosphonium salt remains at a composition except for the stoichiometric composition.

The crystal structure of TBP-DC SCH samples was analyzed by powder X-ray diffraction (PXRD). The samples for PXRD measurements were prepared from aqueous solutions with stoichiometric composition to obtain the crystals without metastable phases. The PXRD patterns were measured at 150 K and atmospheric pressure by use of a diffractometer (PANalytical, X'Pert-MPD) with a cold stage (Anton Paar, TTK450) and Cu  $K\alpha$  X-ray (45 kV, 40 mA). The PXRD measurements were performed in the stepscan mode with a scan rate of 2.7 deg·min<sup>-1</sup> and a step size of approximately 0.02 deg.

The dissociation enthalpies of TBP-DC SCHs were measured by a micro differential scanning calorimeter (Setaram,  $\mu$ DSC VII evo) at atmospheric pressure. Approximately 20 mg of the prepared TBP-DC aqueous solution was loaded into a DSC cell. The precise mass of the loaded aqueous solutions was measured with the electric balance (A&D, BM-22) with an uncertainty of 0.02 mg. The furnace temperature was decreased to 248 K at the cooling rate of 0.5 K·min<sup>-1</sup> and then increased to a desired temperature at the different heating rate of 0.1 K·min<sup>-1</sup>. We calibrated the  $\mu$ DSC with a dedicated Joule heat calibrator (Setaram, EJ3). In addition, water and naphthalene were adopted as references. The uncertainty in the dissociation enthalpy is less than 3 J·g<sup>-1</sup>.

### 3. Results

#### 3.1. Phase equilibrium relations

The phase equilibrium (temperature  $T$  – composition  $x$ ) relations of TBP-DC SCHs are shown in **Figure 2** and are summarized in **Tables 2–7**. The maximum equilibrium temperatures of TBP-Oxa, -Mal, -Suc, -Glu, -Male, and -Fum SCHs were 283.1 K at  $x = 0.0177$  ( $n = 55$ ), 283.4 K at  $x = 0.0154$  ( $n = 64$ ), 282.7 K at  $x = 0.0157$  ( $n = 63$ ), 287.7 K at  $x = 0.0166$  ( $n = 59$ ), 290.3 K at  $x = 0.0157$  ( $n = 63$ ), and 282.9 K at  $x = 0.0163$  ( $n = 60$ ), respectively, where the stoichiometric composition and hydration number of each SCH were estimated by DSC results. The maximum equilibrium temperature of TBP-Oxa SCH obtained in the present study was slightly higher than the reported data by Miyamoto *et al.*<sup>13</sup>, in which the equilibrium temperature was 282.6 K at  $x = 0.0157$  (**Figure 3**).

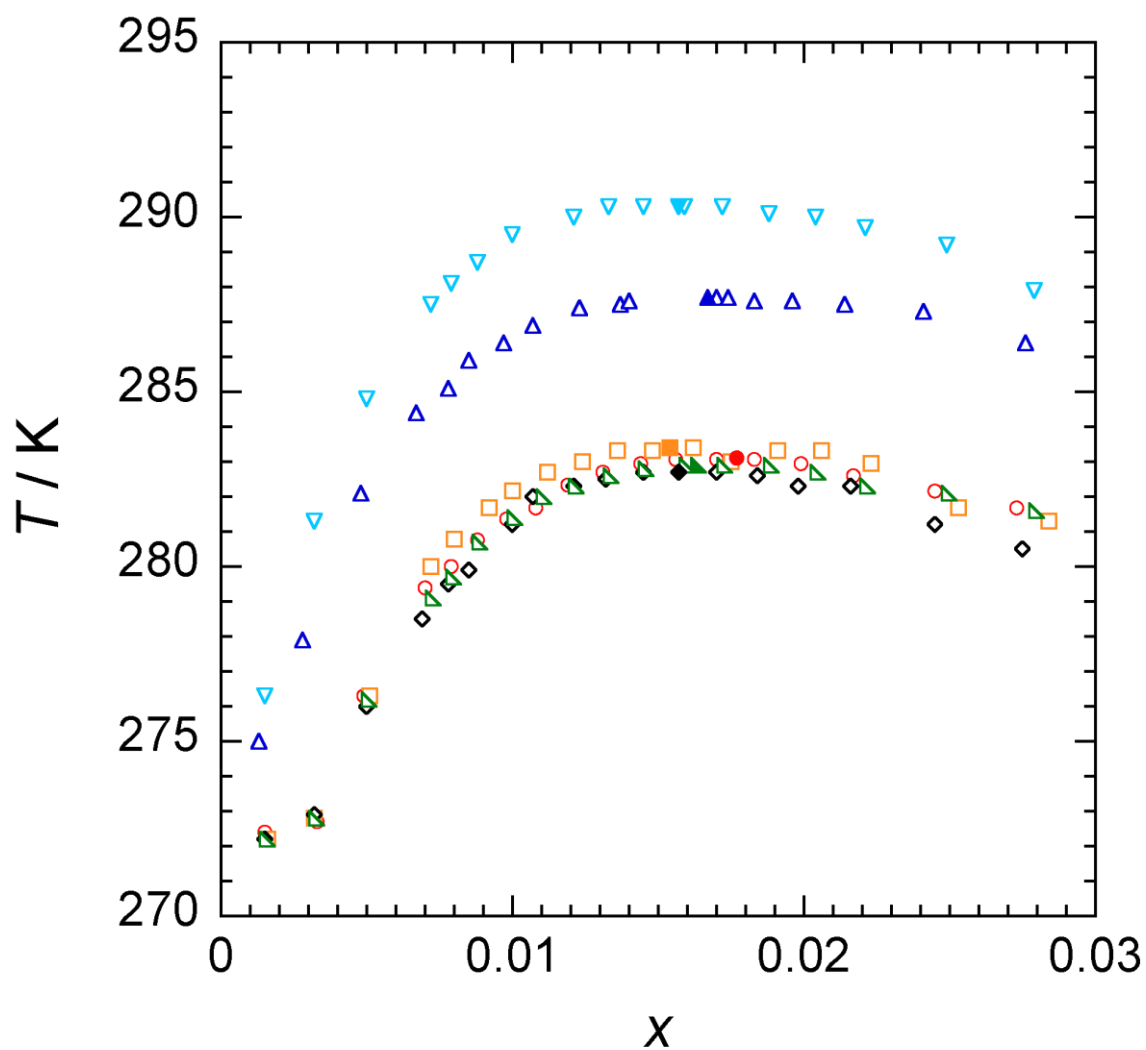


**Figure 2.** Equilibrium temperature ( $T$ )–composition ( $x$ ) diagrams of TBP-Oxa (red circles), TBP-Mal (orange squares), TBP-Suc (black diamonds), TBP-Glu (blue triangle), TBP-Male (light blue inverted triangle) and TBP-Fum (green lower left triangle) SCHs. (For interpretation of the references to color in this figure legend, please see the web version of this article.) Closed keys represent the maximum equilibrium temperatures at stoichiometric compositions determined from the largest apparent dissociation enthalpies.

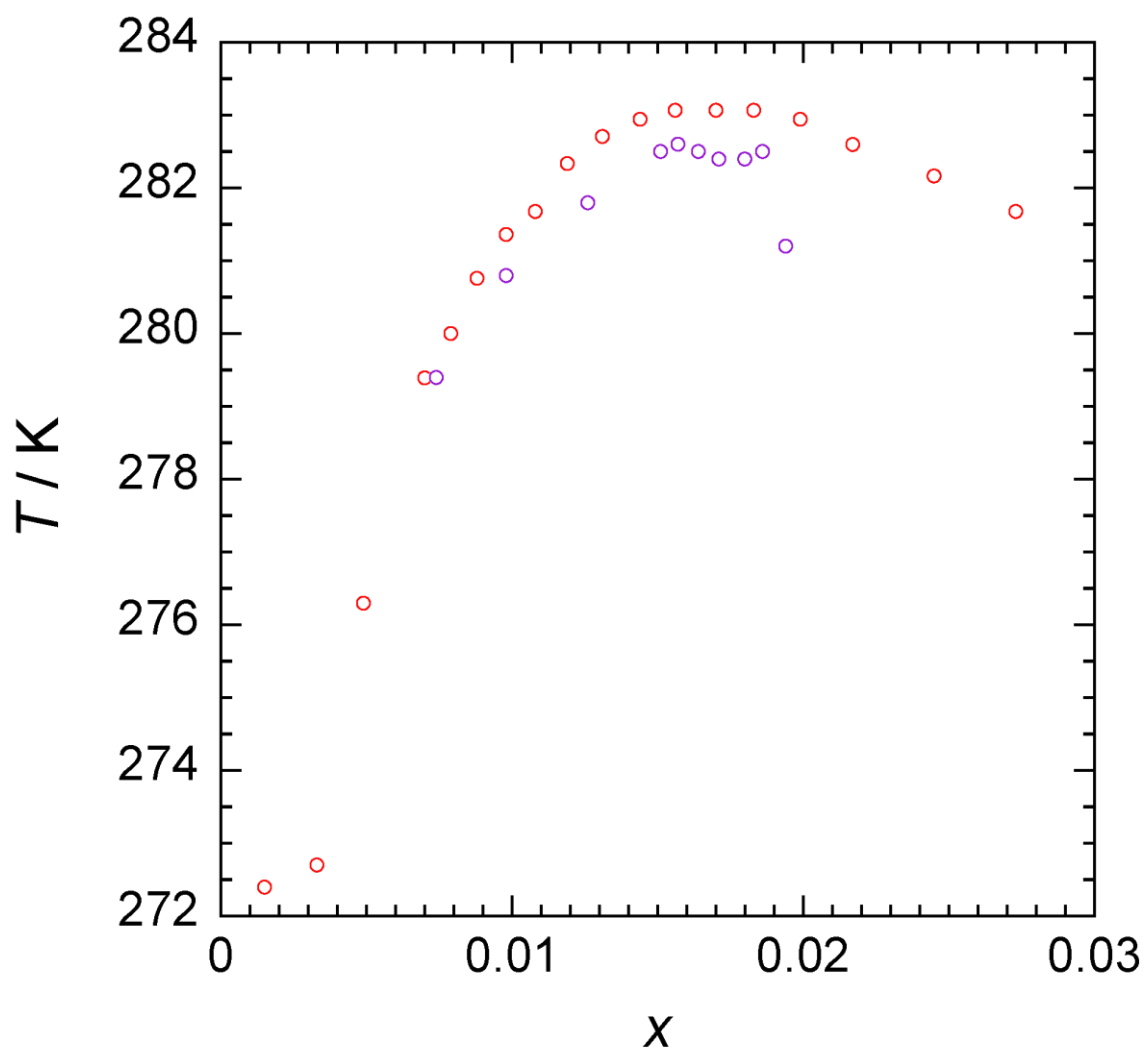


**Figure 3.** Equilibrium temperature ( $T$ )–composition ( $x$ ) diagram of TBP-Oxa SCH in the present study (red circles) with that in ref. 13 (purple circles).

**Table 2.** Equilibrium temperature ( $T$ ) – composition (mole fraction  $x$ , mass fraction  $w$ ) relation of TBP-Oxa SCH (TBP-Oxa, 1; Water, 2).<sup>a</sup>

$x_1$	$w_1$	$T / \text{K}$	$x_1$	$w_1$	$T / \text{K}$
0.0016	0.0498	272.4	0.0152	0.3427	282.9
0.0034	0.1044	272.7	0.0165	0.3606	283.1
0.0051	0.1484	276.3	0.0177 <sup>b</sup>	0.377 <sup>b</sup>	283.1 <sup>b</sup>
0.0074	0.2016	279.4	0.0180	0.3811	283.1
0.0083	0.2208	280.0	0.0194	0.3998	283.1
0.0093	0.2396	280.8	0.0210	0.4198	282.9
0.0104	0.2612	281.4	0.0230	0.4422	282.6
0.0114	0.2804	281.7	0.0259	0.4724	282.2
0.0126	0.3006	282.3	0.0289	0.5004	281.7
0.0139	0.3218	282.7			

<sup>a</sup>Standard uncertainties  $u$  are  $u(x) = 0.0001$ ,  $u(w) = 0.0002$ , and  $u(T) = 0.1 \text{ K}$ .

<sup>b</sup>The maximum equilibrium temperature at the stoichiometric composition that were estimated from the apparent dissociation enthalpies obtained by DSC measurements. The maximum equilibrium temperatures were estimated from the visual observation measurements. At the stoichiometric composition, standard uncertainties  $u$  are  $u(x) = 0.0005$ ,  $u(w) = 0.007$ , and  $u(T) = 0.1 \text{ K}$ .

**Table 3.** Equilibrium temperature ( $T$ ) – composition (mole fraction  $x$ , mass fraction  $w$ ) relation of TBP-Mal SCH (TBP-Mal, 1; Water, 2).<sup>a</sup>

$x_1$	$w_1$	$T / \text{K}$	$x_1$	$w_1$	$T / \text{K}$
0.0016	0.0515	272.2	0.0148	0.3407	283.3
0.0032	0.1007	272.8	0.0154 <sup>b</sup>	0.350 <sup>b</sup>	283.4 <sup>b</sup>
0.0051	0.1496	276.3	0.0162	0.3614	283.4
0.0072	0.1996	280.0	0.0175	0.3805	283.4
0.0080	0.2181	280.8	0.0191	0.4022	283.3
0.0092	0.2417	281.7	0.0206	0.4207	283.3
0.0100	0.2581	282.2	0.0223	0.4404	282.9
0.0112	0.2801	282.7	0.0253	0.4726	281.8
0.0124	0.3026	283.0	0.0284	0.5018	281.3
0.0136	0.3224	283.3			

<sup>a</sup>Standard uncertainties  $u$  are  $u(x) = 0.0001$ ,  $u(w) = 0.0002$ , and  $u(T) = 0.1 \text{ K}$ .

<sup>b</sup>The maximum equilibrium temperature at the stoichiometric composition that were estimated from the apparent dissociation enthalpies obtained by DSC measurements. The maximum equilibrium temperatures were estimated from the visual observation measurements. At the stoichiometric composition, standard uncertainties  $u$  are  $u(x) = 0.0005$ ,  $u(w) = 0.007$ , and  $u(T) = 0.1 \text{ K}$ .



**Table 4.** Equilibrium temperature ( $T$ ) – composition (mole fraction  $x$ , mass fraction  $w$ ) relation of TBP-Suc SCH (TBP-Suc, 1; Water, 2).<sup>a</sup>

$x_1$	$w_1$	$T / \text{K}$	$x_1$	$w_1$	$T / \text{K}$
0.0015	0.0498	272.2	0.0132	0.3208	282.5
0.0032	0.1030	272.9	0.0145	0.3417	282.7
0.0050	0.1513	276.0	0.0157 <sup>b</sup>	0.360 <sup>b</sup>	282.7 <sup>b</sup>
0.0069	0.1957	279.1	0.0170	0.3787	282.7
0.0078	0.2166	279.9	0.0184	0.3984	282.6
0.0085	0.2331	280.7	0.0198	0.4158	282.2
0.0100	0.2616	281.5	0.0216	0.4371	281.1
0.0107	0.2764	281.8	0.0275	0.4994	280.7
0.0121	0.3017	282.3			

<sup>a</sup>Standard uncertainties  $u$  are  $u(x) = 0.0001$ ,  $u(w) = 0.0002$ , and  $u(T) = 0.1 \text{ K}$ .

<sup>b</sup>The maximum equilibrium temperature at the stoichiometric composition that were estimated from the apparent dissociation enthalpies obtained by DSC measurements. The maximum equilibrium temperatures were estimated from the visual observation measurements. At the stoichiometric composition, standard uncertainties  $u$  are  $u(x) = 0.0005$ ,  $u(w) = 0.007$ , and  $u(T) = 0.1 \text{ K}$ .

**Table 5.** Equilibrium temperature ( $T$ ) – composition (mole fraction  $x$ , mass fraction  $w$ ) relation of TBP-Glu SCH (TBP-Glu, 1; Water 2).<sup>a</sup>

$x_1$	$w_1$	$T / \text{K}$	$x_1$	$w_1$	$T / \text{K}$
0.0013	0.0450	275.0	0.0140	0.3386	287.6
0.0028	0.0929	277.9	0.0166 <sup>b</sup>	0.376 <sup>b</sup>	287.7 <sup>b</sup>
0.0048	0.1491	282.1	0.0170	0.3843	287.7
0.0067	0.1963	284.4	0.0174	0.3894	287.7
0.0078	0.2206	285.1	0.0183	0.4014	287.6
0.0085	0.2355	285.9	0.0196	0.4189	287.6
0.0097	0.2601	286.4	0.0214	0.4409	287.5
0.0107	0.2804	286.9	0.0241	0.4710	287.3
0.0123	0.3104	287.4	0.0276	0.5056	286.4
0.0137	0.3336	287.5			

<sup>a</sup>Standard uncertainties  $u$  are  $u(x) = 0.0001$ ,  $u(w) = 0.0002$ , and  $u(T) = 0.1 \text{ K}$ .

<sup>b</sup>The maximum equilibrium temperature at the stoichiometric composition that were estimated from the apparent dissociation enthalpies obtained by DSC measurements. The maximum equilibrium temperatures were estimated from the visual observation measurements. At the stoichiometric composition, standard uncertainties  $u$  are  $u(x) = 0.0005$ ,  $u(w) = 0.007$ , and  $u(T) = 0.1 \text{ K}$ .

**Table 6.** Equilibrium temperature ( $T$ ) – composition (mole fraction  $x$ , mass fraction  $w$ ) relation of TBP-Male SCH (TBP-Male, 1; Water, 2).<sup>a</sup>

$x_1$	$w_1$	$T / \text{K}$	$x_1$	$w_1$	$T / \text{K}$
0.0016	0.0535	276.3	0.0146	0.3422	290.3
0.0031	0.0997	281.3	0.0157 <sup>b</sup>	0.359 <sup>b</sup>	290.3 <sup>b</sup>
0.0048	0.1442	284.8	0.0160	0.3643	290.3
0.0069	0.1960	287.5	0.0171	0.3788	290.3
0.0079	0.2191	288.1	0.0191	0.4067	290.1
0.0088	0.2384	288.7	0.0204	0.4227	290.0
0.0099	0.2596	289.5	0.0217	0.4385	289.7
0.0119	0.2973	290.0	0.0237	0.4600	289.2
0.0142	0.3364	290.3	0.0276	0.4993	287.9

<sup>a</sup>Standard uncertainties  $u$  are  $u(x) = 0.0001$ ,  $u(w) = 0.0002$ , and  $u(T) = 0.1 \text{ K}$ .

<sup>b</sup>The maximum equilibrium temperature at the stoichiometric composition that were estimated from the apparent dissociation enthalpies obtained by DSC measurements. The maximum equilibrium temperatures were estimated from the visual observation measurements. At the stoichiometric composition, standard uncertainties  $u$  are  $u(x) = 0.0005$ ,  $u(w) = 0.007$ , and  $u(T) = 0.1 \text{ K}$ .

**Table 7.** Equilibrium temperature ( $T$ ) – composition (mole fraction  $x$ , mass fraction  $w$ ) relation of TBP-Fum SCH (TBP-Fum, 1; Water, 2).<sup>a</sup>

$x_1$	$w_1$	$T / \text{K}$	$x_1$	$w_1$	$T / \text{K}$
0.0015	0.0502	272.2	0.0145	0.3407	282.8
0.0032	0.1004	272.8	0.0159	0.3618	282.9
0.0050	0.1498	276.2	0.0163 <sup>b</sup>	0.368 <sup>b</sup>	282.9 <sup>b</sup>
0.0072	0.2039	279.1	0.0172	0.3804	282.9
0.0079	0.2183	279.7	0.0188	0.4027	282.9
0.0088	0.2380	280.7	0.0204	0.4222	282.7
0.0100	0.2622	281.4	0.0221	0.4427	282.3
0.0110	0.2810	282.0	0.0249	0.4733	282.1
0.0121	0.3015	282.3	0.0279	0.5022	281.6
0.0133	0.3210	282.6			

<sup>a</sup>Standard uncertainties  $u$  are  $u(x) = 0.0001$ ,  $u(w) = 0.0002$ , and  $u(T) = 0.1$  K.

<sup>b</sup>The maximum equilibrium temperature at the stoichiometric composition that were estimated from the apparent dissociation enthalpies obtained by DSC measurements. The maximum equilibrium temperatures were estimated from the visual observation measurements. At the stoichiometric composition, standard uncertainties  $u$  are  $u(x) = 0.0005$ ,  $u(w) = 0.007$ , and  $u(T) = 0.1$  K.

### 3.2. Crystal structure analysis

PXRD patterns of the TBP-DC SCHs measured at 150 K are shown in **Figure 4**. TBP-Oxa and TBP-Glu SCHs have the same crystal structure. The crystal structure of TBP-Mal, -Suc, -Male, and -Fum SCHs would be the same because of the similarity of their PXRD patterns. The lattice parameters of TBP-DC SCHs were estimated by using the crystallographic data of tetra-*n*-butylammonium dicarboxylate (TBA-DC) SCHs reported by Dyadin *et al.*<sup>19</sup> The obtained PXRD data of TBP-DC SCHs were comparable with the reported crystallographic data of TBA-DC SCHs. The obtained results are summarized in **Table 8**. TBA-Oxa SCH and TBA-Glu SCH have cubic structures with the space group *Im3m* and unit cell parameter of  $a = 2.46$  nm, and *Pm3m* and unit cell parameter of  $a = 2.45$  nm, respectively. TBA-Mal SCH and TBA-Suc SCH have a tetragonal structure with the space group *P4/mmm* and unit cell parameters of  $a = 2.36$  nm and  $c = 1.25$  nm for TBA-Mal SCH, and  $a = 2.36$  nm and  $c = 1.26$  nm for TBA-Suc SCH. There would be no report regarding SCHs based on maleate and fumarate, which have a carbon-carbon double bond of a hydrocarbon chain between carboxyl groups.

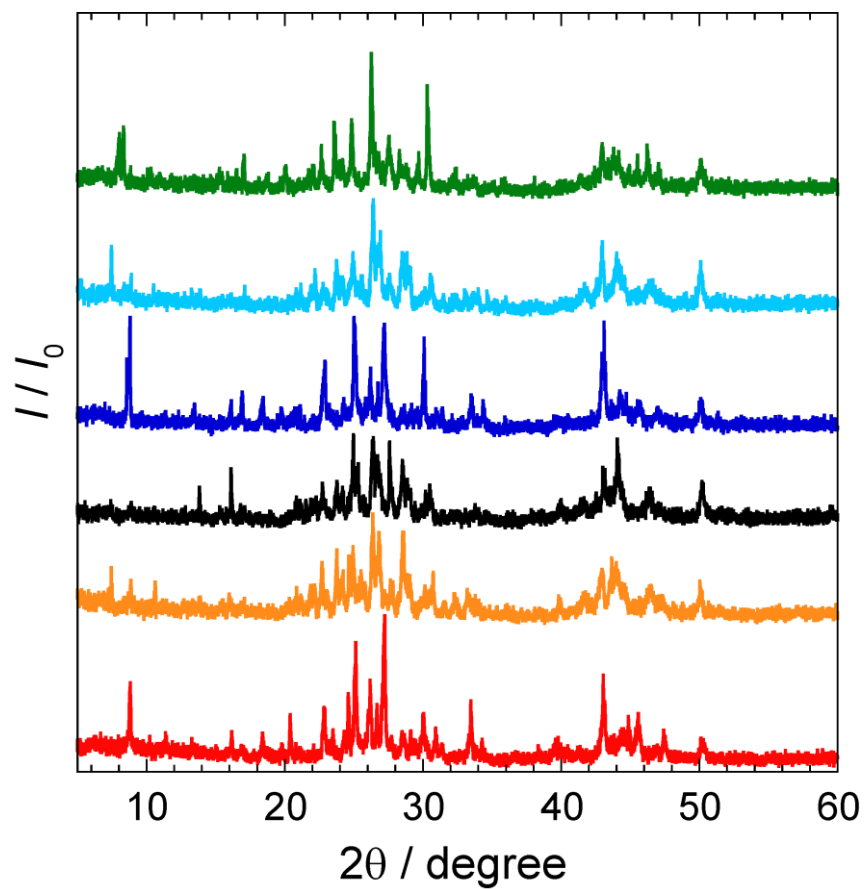


**Figure 4.** PXRD patterns of TBP-Oxa (red line), TBP-Mal (orange line), TBP-Suc (black line), TBP-Glu (blue line), TBP-Male (light blue line), and TBP-Fum (green line) recorded at 150 K and atmospheric pressure.

**Table 8.** Crystal structure and lattice parameter of TBP-DC SCHs measured at 150 K.<sup>a</sup>

SCH	Crystal structure	Lattice parameter	
		<i>a</i> / nm	<i>c</i> / nm
TBP-Oxa	cubic	2.452	-
TBP-Mal	tetragonal	2.361	1.250
TBP-Suc	tetragonal	2.359	1.247
TBP-Glu	cubic	2.448	-
TBP-Male	tetragonal	2.357	1.246
TBP-Fum	tetragonal	2.357	1.247

<sup>a</sup>Standard uncertainties *u* are  $u(a) = 0.001$  nm and  $u(c) = 0.001$  nm.

### 3.3. Dissociation enthalpy and equilibrium temperature measured by DSC

The dissociation enthalpies ( $\Delta_d H$ ) of TBP-DC SCHs were measured by DSC. Typical DSC thermograms of each TBP-DC SCH at the heating rate of  $0.1 \text{ K}\cdot\text{min}^{-1}$  are shown in **Figure 5**, and dissociation enthalpies are listed in **Table 9**.

The dissociation enthalpies of TBP-Oxa, -Mal, -Suc, -Glu, -Male, and -Fum SCHs were 192, 194, 192, 209, 209, and 183  $\text{J}\cdot\text{g}^{-1}$  at the stoichiometric compositions, respectively. Their dissociation enthalpies were suitable for the thermal storage materials because the values were comparable to those

of the typical halide-based SCHs.<sup>2,3,6,7</sup>

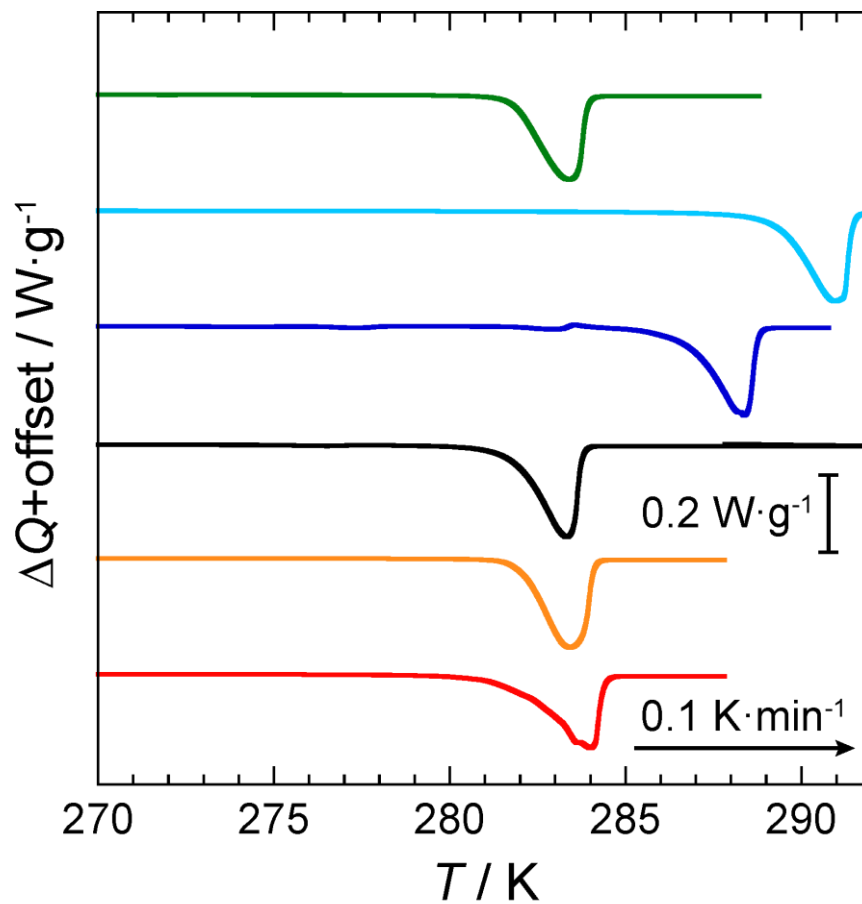


**Figure 5.** Typical DSC thermograms (heat flow  $\Delta Q$ , temperature  $T$ ) of the TBP-Oxa SCH; red line, TBP-Mal SCH; orange line, TBP-Suc SCH; black line, TBP-Glu SCH; blue line, TBP-Male SCH; light blue line, and TBP-Fum SCH; green line at a heating rate of  $0.1 \text{ K} \cdot \text{min}^{-1}$ .



**Table 9.** Dissociation enthalpy  $\Delta_d H$  and hydration number  $n$  of the TBP-DC (1) + water (2) systems.<sup>a</sup>

Compound	$x_1$	$w_1$	$\Delta_d H / \text{J}\cdot\text{g}^{-1}$	$n$
TBP-Oxa	0.0177	0.377	192	55
TBP-Mal	0.0154	0.350	194	64
TBP-Suc	0.0157	0.360	192	63
TBP-Glu	0.0166	0.376	209	59
TBP-Male	0.0157	0.359	209	63
TBP-Fum	0.0163	0.368	183	60

<sup>a</sup>Standard uncertainties  $u$  are  $u(x) = 0.0005$ ,  $u(w) = 0.007$ ,  $u(H) = 3 \text{ J}\cdot\text{g}^{-1}$ , and  $u(n) = 2$ .

#### 4. Discussion

The equilibrium temperatures of TBP-DC SCHs that have various methylene chains without carbon-carbon double bond are plotted in **Figure 6** accompanied with the equilibrium temperatures of corresponding TBA-DC SCHs. The equilibrium temperatures of TBP-Oxa, -Mal, and -Suc SCHs were similar. On the other hand, TBP-Glu SCH showed the highest equilibrium temperature of four TBP-DC SCHs. Also in the case of TBA-DC SCH systems, TBA-Glu SCH exhibits similar trend<sup>19-21</sup>. The reason for equilibrium temperatures of TBP-DC SCHs lower than those of TBA-DC ones may be attributed to the difference in the electrostatic interactions of dicarboxylate anions with phosphonium or ammonium cations<sup>8</sup>, and/or the slight difference in the size of the hydrate cages<sup>4</sup>.

It has been reported that the water molecules are replaced with oxygen atoms of a carboxylate anion in hydrate cages<sup>18, 22-26</sup>. Aladko *et al.* explained that how the oxygen atoms of a carboxyl groups are substituted for the water molecules is important to determine the thermodynamic stability in TBA-DC SCHs, *i.e.*, the thermodynamic stability strongly depends on the methylene length between both carboxyl groups.<sup>21</sup> Especially, glutarate anion has the most appropriate methylene length, since the equilibrium temperature of TBP-Glu SCH is the highest of four TBP-DC SCHs. Dicarboxylate anions having methylene chains longer than glutarate one in TBA-DC SCH systems, the equilibrium temperatures were lowered.<sup>19-21</sup> Similar trend should be considered for the TBP-DC SCH systems.

In the case of dicarboxylate anions with a carbon-carbon double bond of hydrocarbon chain between carboxyl groups, the equilibrium temperature of TBP-Male SCH (290.3 K) was much higher than that of TBP-Fum SCH (282.9 K). Maleate anion takes only *cis* conformation, whereas fumarate anion also takes only *trans* one, because of the rotation restriction derived from the double bonds. These steric conformations should affect how the water molecules are replaced with oxygen atoms of carboxyl groups. The results suggest that the maleate anion with *cis* conformation is more suitable for replacement of water molecules than fumarate anion with *trans* conformation. On the other hand, the equilibrium temperature of SCH based on succinate anion without a double bond was 282.7 K, which was similar to the TBP-Fum SCH one. It is considered that the succinate anion would be in the “*trans*”-like conformation in the hydrate cages, which would result from the electrical repulsion between

carboxyl groups at the ends of the succinate anion (without a double bond). As shown in **Figure 5**, no dissociation peak in the TBP-Suc SCH system was observed near the dissociation temperature (290.3 K) of TBP-Male SCH.

To investigate the conformation of guest substances indirectly, crystal growth of TBP-Suc SCH was observed by adding either a seed crystal of TBP-Male SCH or TBP-Fum SCH. Each seed crystal was prepared from the solutions of stoichiometric composition in the refrigerator kept at 250 K. When the TBP-Fum (*trans*-form) SCH was added as a seed crystal to the supercooled TBP-Suc aqueous solution at the degree of supercooling of 3.3 K, TBP-Suc SCH growth immediately started. The TBP-Male (*cis*-form) SCH did not play the role of a seed crystal for the TBP-Suc SCH growth under the same temperature condition. These results also imply that the conformation of succinate anion would be *trans*-like.

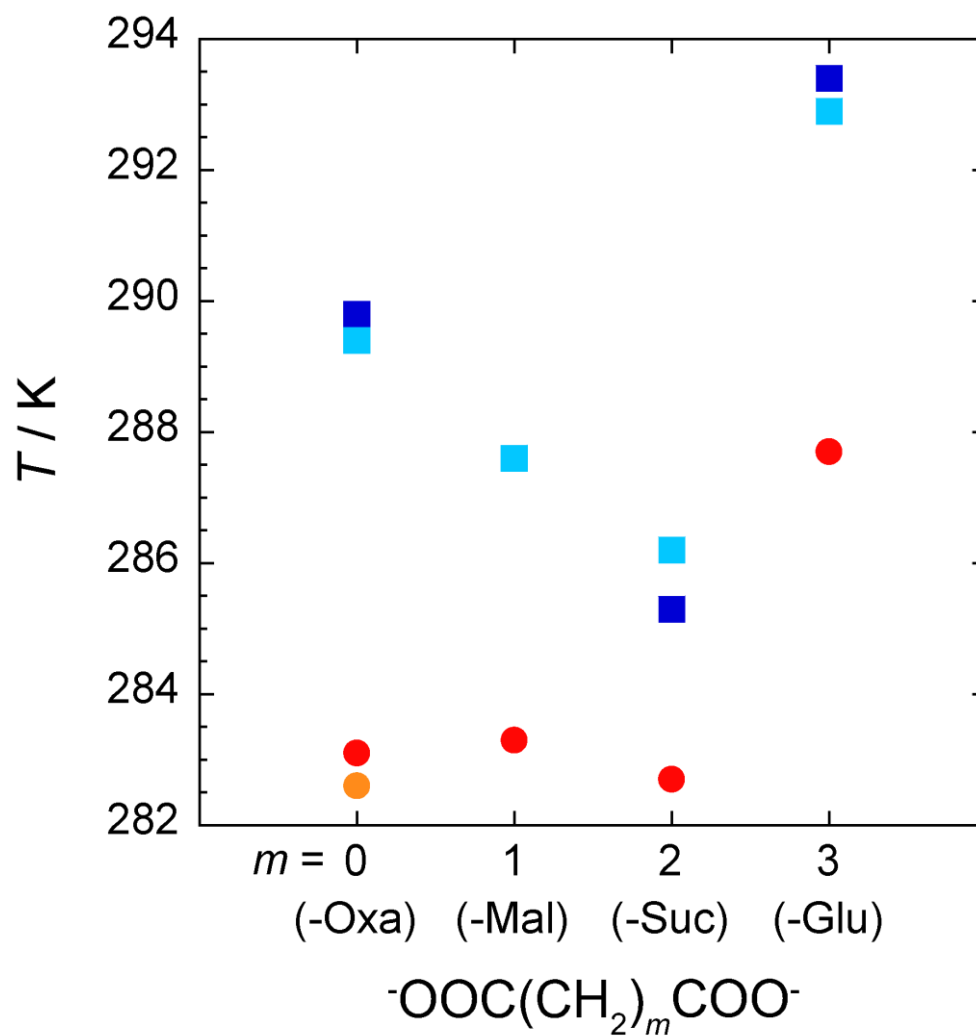


**Figure 6.** The equilibrium temperatures ( $T$ ) of TBP-DC SCHs (red circles, present study), TBA-DC SCHs (blue<sup>19,21</sup> and light blue<sup>20</sup> squares), and the reported data of TBP-Oxa SCH (orange circles, ref. [13]).

## Conclusion

The equilibrium temperatures of TBP-DC SCHs depended on the methylene length and conformation of dicarboxylate anions. In the anion systems without carbon-carbon double bond of hydrocarbon chain between carboxyl groups, the equilibrium temperatures of TBP-Oxa, -Mal, -Suc, and -Glu SCHs were 283.1 K, 283.4 K, 282.7 K, 287.7 K, respectively. The length of methylene chain in the glutarate anion is the most appropriate for the replacement of the water molecules with the oxygen atoms of carboxyl groups. In the anion systems with double bond, the equilibrium temperatures of TBP-Male SCH and TBP-Fum SCH were 290.3 K and 282.9 K, respectively. These results suggested that the maleate with *cis* conformation is more suitable for replacement of the water molecules than the fumarate with *trans* conformation. From the comparison of equilibrium temperature, it is considered that the succinate anion, without double bond, would be in the state of *trans* conformation in the hydrate cages since the equilibrium temperature of TBP-Suc SCH is similar with TBP-Fum one with *trans* conformation. The dissociation enthalpies of TBP-Oxa, -Mal, -Suc, -Glu, -Male, -Fum SCHs were 192, 194, 192, 209, 209, and 183 J·g<sup>-1</sup>, respectively. The difference in equilibrium temperatures caused by steric conformations of guest anions will lead to development of a new thermal storage material or technology of switching equilibrium temperatures by photoisomerization.

## Acknowledgment

This work was supported by JSPS KAKENHI Grant Number JP21J20788 for J.S., JP17H06456 for A.T., JP18K05032 for T.S., and JP19K05412 for K.T. We acknowledge scientific support from the Gas-Hydrate Analyzing System (GHAS) of the Division of Chemical Engineering, Department of Materials Engineering Science, Graduate School of Engineering Science, Osaka University.

## References

- (1) Shimada, W.; Shiro, M.; Kondo, H.; Takeya, S.; Oyama, H.; Ebinuma, T.; Narita, H. Tetra-*n*-butylammonium bromide-water (1/38). *Acta Crystallographica Section C* **2005**, C61, o65-o66.
- (2) Rodionova, T.; Komarov, V.; Villevald, G.; Aladko, L.; Karpova, T.; Manakov, A. Calorimetric and Structural Studies of Tetrabutylammonium Chloride Ionic Clathrate Hydrates. *J. Phys. Chem. B* **2010**, 114, 11838–11846.
- (3) Rodionova, T. V.; Komarov, V. Y.; Villevald, G. V.; Karpova, T. D.; Kuratieva, N. V.; Manakov, A. Y. Calorimetric and Structural Studies of Tetrabutylammonium Bromide Ionic Clathrate Hydrates. *J. Phys. Chem. B* **2013**, 117, 10677-10685.
- (4) Muromachi, S.; Takeya, S.; Yamamoto, Y.; Ohmura, R. Characterization of tetra-*n*-butylphosphonium bromide semiclathrate hydrate by crystal structure analysis. *CrystEngComm* **2014**, 16, 2056-2060.

- (5) Sakamoto, H.; Sato, K.; Shiraiwa, K.; Takeya, S.; Nakajima, M.; Ohmura, R. Synthesis, characterization and thermal-property measurements of ionic semi-clathrate hydrates formed with tetrabutylphosphonium chloride and tetrabutylammonium acrylate. *RSC Advances* **2011**, *1*, 315-322.
- (6) Oshima, M.; Kida, M.; Jin, Y.; Nagao, J. Dissociation behavior of (tetra-*n*-butylammonium bromide + tetra-*n*-butylammonium chloride) mixed semiclathrate hydrate systems. *J. Chem. Thermodynamics* **2015**, *90*, 277-281.
- (7) Sugahara, T.; Machida, H. Dissociation and nucleation of tetra-*n*-butyl ammonium bromide semi-clathrate hydrates at high pressure. *J. Chem. Eng. Data* **2017**, *62*, 2721-2725.
- (8) Shimada, J.; Shimada, M.; Sugahara, T.; Tsunashima, K.; Tani, A.; Tsuchida, Y.; Matsumiya, M. Phase Equilibrium Relations of Semiclathrate hydrates Based on Tetra-*n*-butylphosphonium Formate, Acetate, and Lactate. *J. Chem. Eng. Data* **2018**, *63*, 3615-3620.
- (9) Shimada, J.; Shimada, M.; Sugahara, T.; Tsunashima, K.; Tani, A.; Tsuchida, Y.; Matsumiya, M. Phase equilibrium relations of tetra-*n*-butylphosphonium propionate and butyrate semiclathrate hydrates. *Fluid Phase Equilibria* **2019**, *485*, 61-66.
- (10) Sugahara, T.; Machida, H.; Muromachi, S.; Tenma, N. Thermodynamic properties of tetra-*n*-butylammonium 2-ethylbutyrate semiclathrate hydrate for latent heat storage. *Int. J. Refrig.* **2019**, *106*, 113-119.

- (11) Arai, Y.; Koyama, R.; Endo, F.; Hotta, A.; Ohmura, R. Thermophysical property measurements on tetrabutylphosphonium sulfate ionic semiclathrate hydrate consisting of the bivalent anion. *J. Chem. Thermodynamics* **2019**, 131, 330-335.
- (12) Koyama, R.; Hotta, A.; Ohmura, R. Equilibrium temperature and dissociation heat of tetrabutylphosphonium acrylate (TBPAc) ionic semi-clathrate hydrate as a medium for the hydrate-based thermal energy storage system. *J. Chem. Thermodynamics* **2020**, 144, 106088, 1-8.
- (13) Miyamoto, T.; Koyama, R.; Kurokawa, N.; Hotta, A.; Alavi, S.; Ohmura, R. Thermophysical Property Measurements of Tetrabutylphosphonium Oxalate (TBPOx) Ionic Semiclathrate Hydrate as a Media for the Thermal Energy Storage System. *Front. Chem.* **2020**, 8, 1-10.
- (14) Shimada, J.; Shimada, M.; Sugahara, T.; Tsunashima, K.; Takaoka, Y.; Tani, A. Phase equilibrium temperature and dissociation enthalpy in the tri-*n*-butylphosphonium bromide semiclathrate hydrate systems. *Chem. Eng. Sci.* **2021**, 236, 116514, 1-8.
- (15) Nakayama, H.; Watanabe, K. Hydrates of Organic Compounds. II. The Effect of Alkyl Groups on the Formation of Quaternary Ammonium Fluoride Hydrates. *Bull. Chem. Soc. Jpn* **1976**, 49, 1254-1256.
- (16) Dyadin, Y. A.; Udachin, K. A. Clathrate polyhydrates of peralkylonium salts and their analogs. *J. Struct. Chem.* **1987**, 28, 394-432.



- (17) Nakayama, H.; Usui, H. The effect of carboxylate anions on the formation of clathrate hydrates of tetrabutylammonium carboxylates. *J. Inclusion Phenomena* **1984**, *2*, 249-257.
- (18) Muromachi, S.; Kida, M.; Takeya, S.; Yamamoto, Y.; Ohmura, R. Characterization of the ionic clathrate hydrate of tetra-*n*-butylammonium acrylate. *Can. J. Chem.* **2015**, *93*, 954-959.
- (19) Dyadin, Y. A.; Gaponenko, L. A.; Aladko, L. S.; Bogatyryova, S. V. Clathrate Hydrates of Tetrabutylammonium Carboxylates and Diacboxylates. *J. Inclusion Phenomena* **1984**, *2*, 259-266.
- (20) Nakayama, H.; Watanabe, K. Hydrates of Organic Compounds. III. The Formation of Clathrate-like Hydrates of Tetrabutylammonium Dicarboxylates. *Bull. Chem. Soc. Jpn* **1978**, *51*, 2518-2522.
- (21) Aladko, L. S.; Dyadin, Y. A. Clathrate Hydrates of Tetrabutylammonium Dicarboxylates. System Tetrabutylammonium Adipate-Water. *Russian Journal of General Chemistry* **2004**, *74*, 214-216.
- (22) Rodionova, T.; Komarov, V.; Lipkowski, J.; Kuratieva, N. The structure of the ionic clathrate hydrate of tetrabutylammonium valerate  $(C_4H_9)_4NC_4H_9CO_2 \cdot 39.8H_2O$ . *New J. Chem.* **2010**, *34*, 432-438.
- (23) Komarov, V. Y.; Rodionova, T. V.; Suwinska, K. Single Crystal X-ray Diffraction Study of the Cubic Ionic Clathrate Hydrate of Tetrabutyl Ammonium Propionate  $(C_4H_9)_4NC_2H_5COO \cdot 27.0H_2O$ . *J. Struct. Chem.* **2012**, *53*, 768-775.
- (24) Muromachi, S.; Abe, T.; Yamamoto, Y.; Takeya, S. Hydration structures of lactic acid:

characterization of the ionic clathrate hydrate formed with a biological organic acid anion.

*Phys.Chem.Chem.Phys.*, **2014**, 16, 21467-21472.

(25) Muromachi, S.; Kamo, R.; Abe, T.; Hiaki, T.; Takeya, S. Thermodynamic stabilization of semiclathrate hydrates by hydrophilic group. *RSC Adv.*, **2017**, 7, 13590-13594.

(26) Muromachi, S.; Takeya, S. Thermodynamic Properties and Crystallographic Characterization of Semiclathrate Hydrates Formed with Tetra-*n*-butylammonium Glycolate. *ACS Omega* **2019**, 4, 7317-7322.

TOC

Max. equilib. temp. of TBP-dicarboxylate SCHs

